Heavy-flavour production in Pb–Pb collisions at the LHC, measured with the ALICE detector

Andrea Dainese, for the ALICE Collaboration

INFN – Sezione di Padova, Padova, Italy

E-mail: andrea.dainese@pd.infn.it

Abstract. We present the first results from the ALICE experiment on the nuclear modification factors for heavy-flavour hadron production in Pb–Pb collisions at $\sqrt{s_{\rm NN}} = 2.76$ TeV. Using proton–proton and lead–lead collision samples at $\sqrt{s} = 7$ TeV and $\sqrt{s_{\rm NN}} = 2.76$ TeV, respectively, nuclear modification factors $R_{\rm AA}(p_{\rm t})$ were measured for D mesons at central rapidity (via displaced decay vertex reconstruction), and for electrons and muons, at central and forward rapidity, respectively.

1. Introduction

The ALICE experiment [1] studies nucleus–nucleus and proton–proton collisions at the Large Hadron Collider (LHC), with the main goal of investigating the properties of the high-density, colour-deconfined, state of strongly-interacting matter that is expected to be formed in Pb–Pb collisions. The first Pb–Pb data were collected in November 2010 at a centre-of-mass energy $\sqrt{s_{\rm NN}} = 2.76$ TeV per nucleon–nucleon collision.

Heavy-flavour particles, abundantly produced at LHC energies, are regarded as effective probes of the conditions of the system (medium) formed in nucleus–nucleus collisions:

- open charm and beauty hadrons should be sensitive to the energy density, through the mechanism of in-medium energy loss of heavy quarks;
- quarkonium states should be sensitive to the initial temperature of the system, through their dissociation due to colour screening.

The first ALICE results on charmonium production in Pb–Pb collisions are described in [2]. In this report we present first measurements of the medium-induced suppression of high transverse momentum ($p_{\rm t}$) heavy-flavour hadrons.

The nuclear modification factor $R_{\rm AA}$ of particle $p_{\rm t}$ distributions is well-established as a sensitive observable for the study of the interaction of hard partons with the medium. This factor is defined as the ratio of the $p_{\rm t}$ spectrum measured in nucleus–nucleus (AA) to that expected on the basis of the proton–proton spectrum scaled by the number $N_{\rm coll}$ of binary nucleon–nucleon collisions in the nucleus–nucleus collision:

$$R_{\rm AA}(p_{\rm t}) = \frac{1}{\langle N_{\rm coll} \rangle} \cdot \frac{{\rm d}N_{\rm AA}/{\rm d}p_{\rm t}}{{\rm d}N_{\rm pp}/{\rm d}p_{\rm t}} = \frac{1}{\langle T_{\rm AA} \rangle} \cdot \frac{{\rm d}N_{\rm AA}/{\rm d}p_{\rm t}}{{\rm d}\sigma_{\rm pp}/{\rm d}p_{\rm t}} \,, \qquad (1)$$

where the AA spectrum corresponds to a given collision-centrality class and $\langle T_{\rm AA}\rangle$ is the average nuclear overlap function resulting for that centrality class from the Glauber model of the collisions geometry [3]. A strong suppression in the $R_{\rm AA}$ of charged particles was observed in Pb–Pb collisions at the LHC [4]. Due to the QCD nature of parton energy loss, quarks are predicted to lose less energy than gluons (that have a higher colour charge) and, in addition, the 'dead-cone effect' and other mechanisms are expected to reduce the energy loss of massive quarks with respect to light partons (light-flavour quarks and gluons) [5, 6, 7]. Therefore, one should observe a pattern of gradually decreasing $R_{\rm AA}$ suppression when going from the mostly gluon-originated light-flavour hadrons (e.g. pions) to D and to B mesons [8]: $R^{\pi}_{\rm AA} < R^{\rm D}_{\rm AA} < R^{\rm B}_{\rm AA}$. The measurement and comparison of these different medium probes provide a unique test of the colour-charge and mass dependence of parton energy loss.

The ALICE experiment was designed to detect heavy-flavour hadrons over a wide phase-space coverage and in various decay channels, as we will discuss in section 2. The production of heavy-flavour probes was measured in proton–proton collisions at $\sqrt{s} = 7$ TeV and compared to perturbative QCD (pQCD) predictions. These results, reported in section 3, provide a well-defined, calibrated, reference for $R_{\rm AA}$ measurements. The reference at the Pb–Pb $\sqrt{s_{\rm NN}}$ energy is obtained by a pQCD-driven scaling (section 4). The Pb–Pb analysis results and the nuclear modification factors of $\rm D^0$ and $\rm D^+$ mesons, and of electrons and muons from heavy-flavour decays are presented in section 5. More details on these analyses can be found in [9, 10, 11, 12].

2. Heavy-flavour production measurements in ALICE

The heavy-flavour detection capability of the ALICE detector, described in detail in [1], is mainly provided by:

- Tracking system; the silicon Inner Tracking System (ITS) and the Time Projection Chamber (TPC) embedded in a magnetic field of 0.5 T, allow track reconstruction in the pseudo-rapidity range $|\eta| < 0.9$ with a momentum resolution better than 4% for $p_{\rm t} < 20$ GeV/c and a transverse impact parameter‡ resolution better than 75 μm for $p_{\rm t} > 1$ GeV/c with a high-$p_{\rm t}$ saturation value of 20 μm.
- Particle identification system; charged hadrons are separated via their specific energy deposit $\mathrm{d}E/\mathrm{d}x$ in the TPC and via time-of-flight measurement in the Time Of Flight (TOF) detector; electrons are identified at low $p_{\rm t}$ (< 6 GeV/c) via TPC $\mathrm{d}E/\mathrm{d}x$ and time-of-flight, and at intermediate and high $p_{\rm t}$ (> 2 GeV/c) in the dedicated Transition Radiation Detector (TRD) and in the Electromagnetic Calorimeter (EMCAL); muons are identified in the muon spectrometer covering the pseudo-rapidity range $-4 < \eta < -2.5$§.

‡ The transverse impact parameter, d_0, is defined as the distance of closest approach of the track to the interaction vertex, in the plane transverse to the beam direction.

§ Since the colliding particles, pp and Pb–Pb, are symmetric in mass, we indicate the muon spectrometer acceptance using positive values in the following.

The main detection modes are listed below.

- Charm hadronic decays in $|y| < 0.5$ using displaced vertex identification: $\mathrm{D}^0 \to \mathrm{K}^-\pi^+$, $\mathrm{D}^+ \to \mathrm{K}^-\pi^+\pi^+$, and $\mathrm{D}^{*+} \to \mathrm{D}^0\pi^+$. Other channels and hadrons are under study: $\mathrm{D}^0 \to \mathrm{K}^-\pi^+\pi^-\pi^+$, $\mathrm{D}_\mathrm{s}^+ \to \mathrm{K}^-\mathrm{K}^+\pi^+$, and $\Lambda_\mathrm{c}^+ \to \mathrm{pK}^-\pi^+$.
- Leptons from heavy-flavour decays: inclusive $\mathrm{D/B} \to \mathrm{e} + X$ in $|y_\mathrm{e}| < 0.8$ and $\mathrm{D/B} \to \mu + X$ in $2.5 < y_\mu < 4$; $\mathrm{B} \to \mathrm{e} + X$ using displaced electron identification (only in pp for the moment). $\mathrm{B} \to \mathrm{J}/\psi\,(\to \mathrm{e}^+\mathrm{e}^-) + X$ is also under study.

The results that we present are obtained from data recorded with minimum-bias trigger selections in pp and Pb–Pb collisions. These selections were defined by the presence of signals in either of two scintillator hodoscopes, the V0 detectors, positioned in the forward and backward regions of the experiment, or in the silicon pixel barrel detector, in coincidence with the signals of two beam pick-up counters on both sides of the interaction region. For muon analyses in pp collisions, a second selection requests, in addition to the minimum-bias condition, a muon trigger signal ($p_\mathrm{t} > 0.5$ GeV/c). The results presented correspond to about 100–180 million (depending on the analysis) pp minimum-bias triggers and about 17 million Pb–Pb minimum-bias triggers. For pp collisions, the heavy flavour production cross sections are normalized relative to the minimum-bias trigger cross section, which is derived using a van-der-Meer scan technique. Pb–Pb collision-centrality classes are defined in terms of percentiles of the distribution of the sum of amplitudes in the V0 scintillator detectors.

3. Calibrating heavy-flavour probes with pp collisions at $\sqrt{s} = 7$ TeV

The detection strategy for D mesons at central rapidity is based, for both pp and Pb–Pb collisions, on the selection of displaced-vertex topologies, i.e. separation of tracks from the secondary vertex from those from the primary vertex, large decay length (normalized to its estimated uncertainty), and good alignment between the reconstructed D meson momentum and flight-line. The identification of the charged kaon in the TPC and TOF detectors helps to further reduce the background at low p_t. An invariant-mass analysis is then used to extract the raw signal yield, to be then corrected for detector acceptance and for PID, selection and reconstruction efficiency, evaluated from a detailed detector simulation. The contamination of D mesons from B meson decays is estimated to be of about 15%, using the beauty production cross section predicted by the FONLL (fixed-order next-to-leading log) calculation [13] and the detector simulation, and it is subtracted from the measured raw p_t spectrum, before applying the efficiency corrections. The D^0, D^+, and D^{*+} p_t-differential production cross sections in $|y| < 0.5$ are shown in Fig. 1. Theoretical predictions based on pQCD calculations (FONLL [13] and GM-VFNS [14]) are in agreement with the data.

At central rapidity, heavy flavour production is measured also using semi-electronic decays. The basis of this measurement is a robust electron identification. For pp collisions, this uses the signals in the TPC, TOF, and TRD detectors, as detailed in [10] (the EMCAL information will also be exploited in the near future). The residual

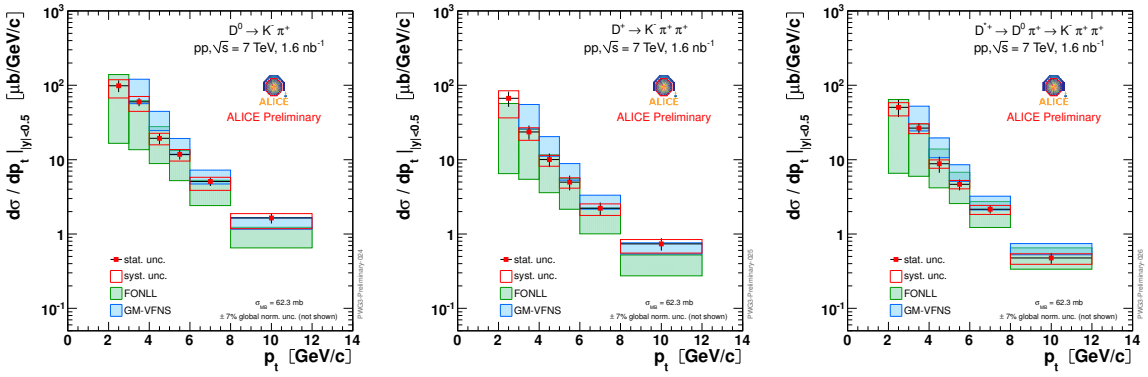

Figure 1. D^0, D^+, and D^{*+} p_t-differential production cross sections in $|y| < 0.5$ in pp collisions at $\sqrt{s} = 7$ TeV, compared to pQCD calculations [13, 14].

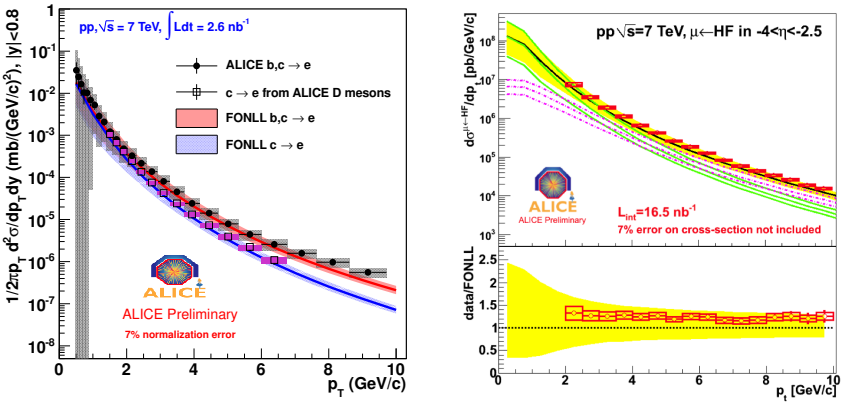

Figure 2. p_t-differential production cross sections of heavy-flavour decay electrons in $|y| < 0.8$ (left) and muons in $2.5 < y < 4$ (right) in pp collisions at $\sqrt{s} = 7$ TeV, compared to pQCD calculations [13]. The left panel shows also the cross section of electrons obtained by applying the decay kinematics to the D cross sections in Fig. 1.

pion contamination in the electron sample is measured, and then subtracted, by fitting with a two component function the TPC $\mathrm{d}E/\mathrm{d}x$ distribution in narrow momentum slices. The p_t-differential cross section of electrons from charm and beauty particle decays is obtained by subtracting from the efficiency-corrected inclusive spectrum a "cocktail" of background electrons. The components of the cocktail are electrons from light-flavour hadron decays (mainly π^0 Dalitz decays, in addition to η, ρ, ω, and ϕ decays), and γ conversions in the beam pipe and innermost pixel layer. These inputs are determined from the measured pion cross section, using simulations and m_t scaling [10]. Figure 2 (left) shows the resulting heavy-flavour decay electrons cross section in $|y| < 0.8$, compared to the corresponding FONLL prediction [13] and to the cross section of charm decay electrons, obtained by applying the decay kinematics to the D cross sections.

Heavy flavour production at forward rapidity is measured using the single-muon p_t

distribution. The extraction of the heavy-flavour contribution from the single muon spectra requires the subtraction of three main sources of background: muons from the decay-in-flight of light hadrons (decay muons); muons from the decay of hadrons produced in the interaction with the front absorber (secondary muons); hadrons that punch through the front absorber. The last contribution, about 20% for $p_{\rm t} > 2$ GeV/c, can be efficiently rejected by requiring the matching of the reconstructed tracks with the tracks in the trigger system. Due to the lower mass of the parent particles, the light-hadron decay muons have a softer transverse momentum than the heavy-flavour muons, and dominate the low-$p_{\rm t}$ region. In the pp analysis this background is subtracted using simulations, as detailed in [12]. The charm and beauty decay muon cross section $\mathrm{d}\sigma/\mathrm{d}p_{\rm t}$ in the range $2.5 < y < 4$ is presented in Fig. 2 (right). The corresponding FONLL [13] prediction agrees with our data and indicates that beauty decays are the dominant contribution for $p_{\rm t} > 6$ GeV/c.

4. pp references at $\sqrt{s} = 2.76$ TeV via pQCD-driven $\sqrt{s}$-scaling

The reference pp cross sections used for the determination of the nuclear modification factors were obtained by applying a $\sqrt{s}$-scaling [15] to the cross sections measured at $\sqrt{s} = 7$ TeV. The scaling factors for each of the three observables (D mesons, muons, electrons) were defined as the ratios of the cross sections from the FONLL pQCD calculation at 2.76 and 7 TeV. The assumption that was made is that the following quantities do not vary with $\sqrt{s}$: a) the pQCD scale values (factorization and renormalization scales) and b) the c and b quark masses used in the calculation. The theoretical uncertainty on the scaling factor was evaluated by considering the envelope of the scaling factors resulting from different values of the scales and heavy quark masses. This uncertainty is similar for D mesons and for heavy-flavour decay leptons at the two rapidities and it ranges from 25% at $p_{\rm t} = 2$ GeV/c to less that 10% above 10 GeV/c [15].

For D mesons, the procedure was validated by scaling the ALICE data to Tevatron energy, $\sqrt{s} = 1.96$ TeV, and comparing [15] to CDF measurements [16].

The D^0 and D^+ cross sections were measured, though with limited precision of 20–25% and $p_{\rm t} < 8$ GeV/c, also for pp collisions at $\sqrt{s} = 2.76$ TeV collected during a short reference run at the same energy as Pb–Pb collisions. These measurements at $\sqrt{s} = 2.76$ TeV were found to be in agreement with the scaled 7 TeV measurements.

5. Heavy-flavour nuclear modification factors in Pb–Pb at $\sqrt{s_{\rm NN}} = 2.76$ TeV

D mesons are reconstructed in Pb–Pb collisions [9] using the same strategy as for the pp case, exploiting the vertexing precision and the hadron identification capabilities of the ALICE detector. The $\mathrm{D}^0 \to \mathrm{K}^-\pi^+$ signal was measured in five $p_{\rm t}$ bins in 2–12 GeV/c and the $\mathrm{D}^+ \to \mathrm{K}^-\pi^+\pi^+$ signal in three bins in 5–12 GeV/c. An example Kπ invariant mass distribution for $p_{\rm t} > 2$ GeV/c in the 0–20% centrality class is shown in Fig. 3 (left). The reconstruction and cut selection efficiency, evaluated from detailed

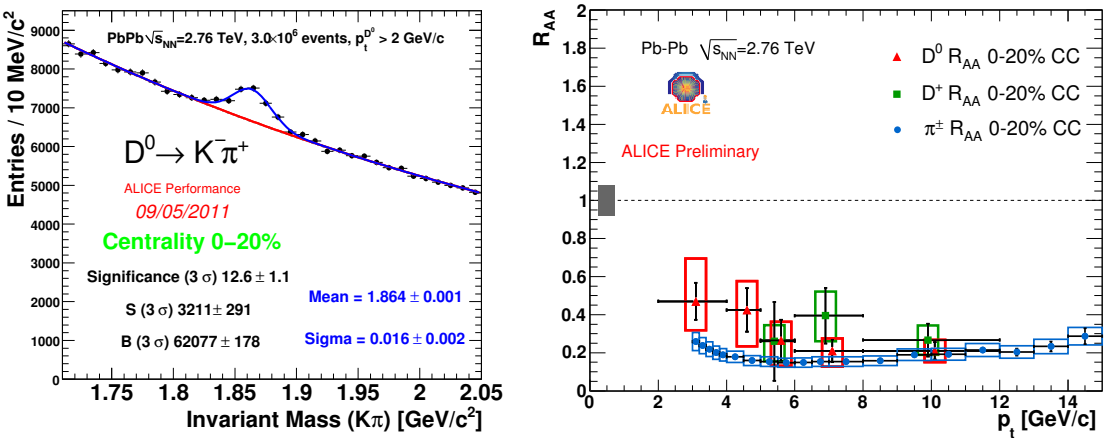

Figure 3. Left: $\mathrm{D}^0 \to \mathrm{K}^-\pi^+$ signal in the Kπ invariant mass distribution for central (0–20%) Pb–Pb. Right: R_{AA} for D^0, D^+, and π^+ in central collisions. Statistical (bars), systematic (empty boxes), and normalization (full box) uncertainties are shown.

detector simulation, ranges between 1 and 10% for increasing p_{t} and it does not show a significant dependence on the collision centrality. The subtraction of feed-down from B meson decays relies on the FONLL predictions, as for the pp case. This contribution is of about 10–15%. The systematic uncertainty related to the FONLL theoretical uncertainty is correlated in the pp and Pb–Pb spectra, thus it partly cancels in the R_{AA} ratio. An additional source of systematic uncertainty arises from the unknown nuclear modification of B meson production. To estimate this uncertainty, the prompt D meson R_{AA} was evaluated for the range of hypotheses $0.3 < R^{\mathrm{B}}_{\mathrm{AA}}/R^{\mathrm{D}}_{\mathrm{AA}} < 3$ and the resulting variation was found to be smaller than 15%. This is relatively small in comparison to the total experimental systematic uncertainty of about 35%, which is dominated by the track reconstruction, particle identification and cut efficiency corrections. The nuclear modification factor of prompt D^0 and D^+ mesons in central (0–20%) Pb–Pb collisions is shown in Fig. 3 (right). A strong suppression is observed, reaching a factor 4–5 for $p_{\mathrm{t}} > 5$ GeV/c for both D meson species. Their R_{AA} is compatible with that of charged pions, also shown, although there seems to be a tendency for $R^{\mathrm{D}}_{\mathrm{AA}} > R^{\pi}_{\mathrm{AA}}$ at low p_{t}.

Like for D mesons, also for single electrons and single muons the Pb–Pb analysis strategy is similar to the pp case. Electron identification is based on the TPC and TOF detector signals only, for the moment, and the electron p_{t} spectra are limited to the region below 6 GeV/c, to keep the hadron contamination below 15% (as in pp, measured from the TPC $\mathrm{d}E/\mathrm{d}x$). The inclusive electron spectra, corrected for efficiency and acceptance, and the background cocktail, based on measured $\pi^{\pm}$ spectra, are extracted in six centrality classes. At variance with pp and peripheral Pb–Pb collisions, for semi-central and central Pb–Pb collisions the comparison with the cocktail shows a hint for an excess of electrons in the low-p_{t} region (up to about 3 GeV/c), that increases towards more central collisions [11]. This could be related to thermal photons

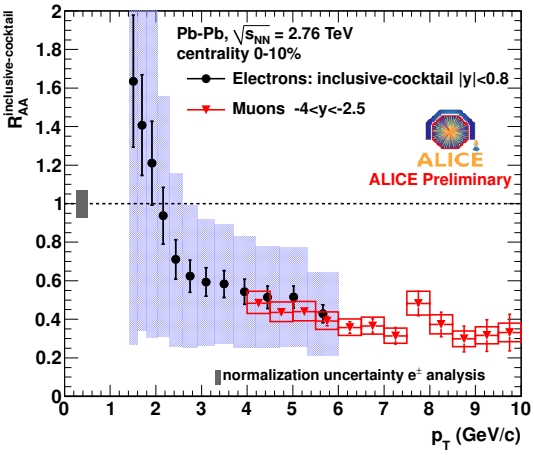

Figure 4. Nuclear modification factors for cocktail-subtracted inclusive electrons at central rapidity and inclusive muons at forward rapidity in central (0–10%) Pb–Pb collisions. Statistical (bars) and systematic (empty boxes) uncertainties are shown.

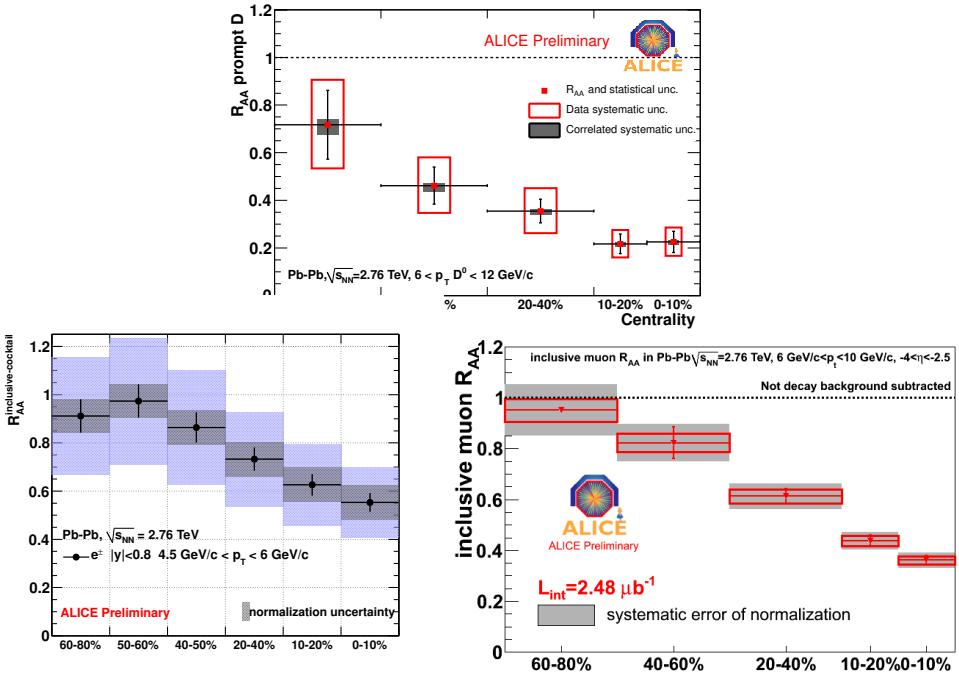

Figure 5. Centrality dependence of $R_{\rm AA}$ for $\rm D^0$ mesons (top) for cocktail-subtracted inclusive electrons at central rapidity (bottom-left), and for inclusive muons at forward rapidity (bottom-right). The $p_{\rm t}$ intervals are indicated in the figures.

radiated by the hot QCD medium. For $p_{\rm t} > 3$–4 GeV/c the background-subtracted inclusive electron spectrum should be dominated by decays of D and B mesons. We use this spectrum to compute $R_{\rm AA}(p_{\rm t})$, which is shown for the 0–10% centrality class in Fig. 4. A suppression of a factor 1.5–4 is observed above 4 GeV/c. The large systematic

uncertainty is dominated by the electron identification corrections. The same figure shows also the $R_{\rm AA}$ of inclusive muons in $2.5 < y < 4$. In Pb–Pb the light-flavour decay muon component is not subtracted as in pp, but we estimated using simulations that this background is smaller than 10–15% for $p_{\rm t} > 6$ GeV/c. The muon $R_{\rm AA}$ shows a suppression of factor about 3 up to 10 GeV/c, in a momentum range where beauty decay muons should be dominant.

Figure 5 shows the centrality dependence of the nuclear modification factors for $\rm D^0$ mesons, single electrons, and single muons, for $p_{\rm t} > 4$ ($\rm e^+$) and 6 (μ^+ and $\rm D^0$) GeV/c. For all three cases, the suppression tends to vanish towards peripheral collisions. The $R_{\rm AA}$ of electrons at central rapidity and of muons at forward rapidity is compatible, while the $R_{\rm AA}$ of prompt D mesons is systematically lower. This feature is present in the predictions of models in which the energy loss is smaller for b than for c quarks [8, 17].

6. Conclusions

The first ALICE results on the $R_{\rm AA}$ nuclear modification factors of heavy-flavour hadrons in Pb–Pb collisions at the LHC imply a strong in-medium energy loss for c and b quarks. The $\rm D^0$ and $\rm D^+$ $R_{\rm AA}$, measured for the first time as a function of $p_{\rm t}$ and centrality, is as low as 0.2–0.3 for $p_{\rm t} > 5$ GeV/c and compatible with the $R_{\rm AA}$ of pions. Below 5 GeV/c, there is an indication for a rise and for $R^{\rm D}_{\rm AA} > R^{\pi}_{\rm AA}$. Higher statistics data, expected from the 2011 Pb–Pb run, and comparison data in p–Pb collisions should allow to study this region with more precision and disentangle the initial-state nuclear effects, which could be different for light and heavy flavours. A large suppression, $R_{\rm AA} \approx 0.3$–0.4, however systematically larger than for D mesons, is observed also for inclusive electrons and muons in the $p_{\rm t}$ range above 5 GeV/c, where beauty decays are dominant according to pQCD calculations. The direct measurement of $R_{\rm AA}$ of electrons from beauty decays should be possible with the data of the 2011 Pb–Pb run.

References

[1] K. Aamodt *et al.* [ALICE Coll.], JINST **3** (2008) S08002.
[2] G. Martinez-Garcia, for the ALICE Coll.; P. Pillot, for the ALICE Coll., these proceedings.
[3] M. Miller, K. Reygers, S. Sanders, and P. Steinberg, Ann. Rev. Nucl. Part. Sci. **57** (2007) 205.
[4] K. Aamodt *et al.* [ALICE Coll.], Phys. Lett **B696** (2011) 30-39.
[5] Y. L. Dokshitzer, D. E. Kharzeev, Phys. Lett. **B519** (2001) 199-206.
[6] N. Armesto, C. A. Salgado, U. A. Wiedemann, Phys. Rev. **D69** (2004) 114003.
[7] S. Wicks, W. Horowitz, M. Djordjevic, M. Gyulassy, Nucl. Phys. **A783** (2007) 493-496.
[8] N. Armesto, A. Dainese, C. A. Salgado, U. A. Wiedemann, Phys. Rev. **D71** (2005) 054027.
[9] A. Rossi, for the ALICE Coll., these proceedings.
[10] S. Masciocchi, for the ALICE Coll., these proceedings.
[11] Y. Pachmayer, for the ALICE Coll., these proceedings.
[12] X. Zhang, for the ALICE Coll., these proceedings.
[13] M. Cacciari, M. Greco, P. Nason, JHEP **9805** (1998) 007; private communication.
[14] B.A. Kniehl *et al.*, Phys. Rev. Lett. **96** (2006) 012001; private communication.
[15] R. Averbeck, N. Bastid, Z. Conesa del Valle, A. Dainese, X. Zhang, arXiv:11073243 (2011).
[16] D. Acosta *et al.* [CDF Coll.], Phys. Rev. Lett. **91** (2003) 241804.
[17] Z. Conesa del Valle *et al.*, Phys. Lett. **B663** (2008) 202-208.